Modular Platform for Mobile Biosensing with Extended Gate Field-Effect Transistors

Jack Twiddy[1], Ethan Cove[2], Hayley Richardson[2,3], Lina Acosta-Perez[1], Mika Hatada[1], Ellie Wilson[1], Koji Sode[1], Spyridon Pavlidis[2], Michael Daniele[1,2]

[1]Joint Department of Biomedical Engineering, NC State University and UNC at Chapel Hill, Raleigh, NC, USA
[2]Department of Electrical & Computer Engineering, NC State University, Raleigh, NC, USA
[3]Department of Materials Science and Engineering, NC State University, Raleigh, NC, USA
mdaniel6@ncsu.edu, spavlidis@ncsu.edu, ksode@email.unc.edu

***Abstract*—We present a modular platform for mobile biosensing using an extended gate field-effect transistor architecture. Our device contains transduction hardware for amplifying changes in electrochemical cell potential in an analyte-agnostic manner and can be interfaced with a wide variety of functionalized electrodes for the detection of any analyte for which a suitable recognition element exists. Here, the device is presented and characterized, and its applicability demonstrated using a panel of example electrode systems for the measurement of picomolar concentrations of neuropeptide Y and insulin, as well as variations in pH.**

Keywords— extended gate field-effect transistor; insulin; neuropeptide Y; potentiometry; mobile

I. Introduction

Electrochemical detection of biomolecules using wearables represents a rapidly growing area of research and commercialization, as the value of longitudinal patient monitoring is increasingly recognized [1-4]. While electrochemical methods are widely applied in clinical laboratories, *e.g.* quantification pH, ion concentration, and dissolved gases in blood [5, 6], detection of toxins [7, 8], determination of coagulation status [9], and blood glucose sensing [10]. Yet, adoption of these techniques in the context of wearable and implantable devices has been comparatively limited. Perhaps the best example of a wearable device utilizing electrochemical detection is continuous glucose monitors [11, 12], which almost universally utilize amperometric detection of hydrogen peroxide, a reporter enzymatically generated from glucose. Ongoing development in the area of wearable electrochemical sensors has focused on the detection of other biomolecules of interest through the creation of new and improved electrode functionalization approaches, as well as the deployment of other electrochemical techniques, which may be more suited to the target analyte and operational sensing matrix.

The extended gate field-effect transistor (EGFET) is an electrochemical sensing architecture originally explored in the 1980s and following decades [13-15] that has seen a surge of recent interest [16-18]. EGFET sensing can be thought of as an extension of open circuit potentiometry (OCP) [19], in which the whole-cell or half-cell potential is measured under electrochemical equilibrium, *i.e.* with zero net current passing through the cell. This potential is indirectly transduced by connecting the working electrode (WE) to the gate of a conventional semiconductor FET (hence "extended gate"), resulting in variations in the measured FET drain current (I_D) in response to fluctuations in the electrochemical cell potential.

There are several advantages to this mode of detection: first, as in OCP sensing, the potentiometric nature of EGFET sensing results in a sensor output which is independent of the physical size of the electrode; second, the FET gate oxide produces an equivalently high input impedance compared to operational amplifier-based potentiometry circuits, while allowing for easier tuning of the output signal magnitude through changes in the bias potentials applied to the FET drain and the counter/reference electrode (RE). EGFET sensors leverage a similar amplification scheme to sensors using electrochemical FETs, but benefit from the improved stability and reproducibility of a discrete semiconductor transistor. While an EGFET sensor generally necessitates an additional current-to-voltage conversion stage to transduce changes in I_D, the overall size and complexity of an EGFET circuit may be less than that of an equivalent OCP-based solution, due to the separation of high-impedance input and gain stages (each requiring an operational amplifier) in the latter case, due to the lower input impedance of an amplifier providing gain through feedback.

While substantial engineering work has targeted development of recognition elements and electrode systems for EGFET sensing, evaluation of these systems in vivo (and their eventual translation to real-world deployment) necessitates the availability of suitable miniaturized supporting electronics. Herein, we report a purpose-built platform for integration of EGFET sensors that provides for both storage and wireless transmission of the resulting data. As our system is intended to be analyte-agnostic and widely applicable when paired with a suitable recognition element/electrode, we demonstrate benchtop quantification of several biomolecules and solution conditions of medical interest, including neuropeptide Y (NPY, a stress biomarker [20]), insulin, and pH change.

II. Materials and Methods

A. Device Architecture

For modularity, the EGFET system consists of three stackable printed circuit boards (PCBs): an "analog frontend" board containing the EGFET transduction circuit and a local low-noise power supply (MCP1754S, Microchip Technology); a "backend" control board containing a wireless microcontroller

This work was supported by the NSF Engineering Research Center for Advanced Self-Powered Systems for Integrated Sensors and Technologies (EEC-1160483), the NC State Institute for Connected Sensor-Systems, the Juvenile Diabetes Research Foundation, and the Helmsley Charitable Trust.

2024 IEEE BioSensors Conference (BioSensors) | 979-8-3503-9513-6/24/$31.00 ©2024 IEEE | DOI: 10.1109/BIOSENSORS61405.2024.10712698

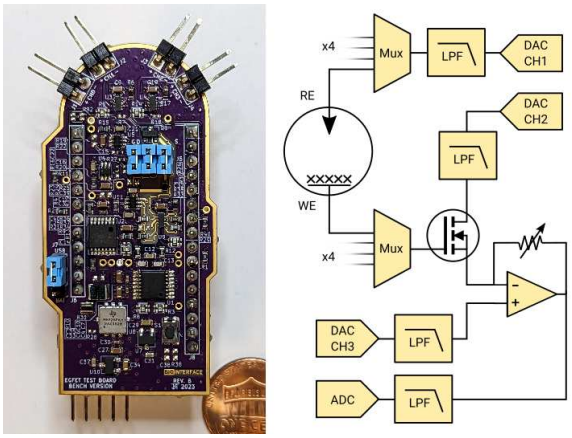

Fig. 1. Photograph of EGFET platform (left) and system diagram showing simplified analog frontend circuit (right).

(ESP32-S2, Espressif), global power management (ADP2504, Analog Devices), and battery management (BQ25303J, Texas Instruments); and an optional data collection support board featuring an SD card receptacle and a real-time clock (RV-3028-C7, Micro Crystal AG) to facilitate local data storage and timestamping. When all three boards are used, the whole device is approximately 62.5 mm x 31.1 mm x 27.5mm.

The analog frontend board (**Fig. 1**) implements the EGFET operation through the combination of an N-channel FET (IRLML6246TRPBF, Infineon Technologies) and an operational amplifier (MAX44260, Maxim Integrated/Analog Devices) configured as a transimpedance amplifier (TIA). A 4:1 analog multiplexer (TMUX1104, Texas Instruments) includes one of four precision resistors in the TIA feedback loop to select between four levels of gain, nominally 5 , 10, 50, or 100 kV/A. Two identical multiplexers provide for connection of up to four independent WE and RE channels each, enabling a wide range of sensing configurations, *e.g.* 4 independent cells, 4 WE to a common RE, etc.). Due to large inter-transistor variability in FET threshold voltage (V_{th}) [21], evaluation of device performance against a lab-grade source-measure unit or potentiostat is facilitated through a set of jumpers, which enable the on-board FET to be fully isolated from the frontend circuit and connected to external equipment. A signal conditioning subcircuit consisting of a DAC (AD5665R, Analog Devices), an ADC (ADS1119, Texas Instruments), and a precision voltage reference (REF7025, Texas Instruments) performs biasing of the electrochemical cell, FET drain, and TIA bias point, as well as digitization of the TIA output. First-order reconstruction filters, buffered in the case of the electrochemical cell and FET drain, and an antialiasing filter limit system bandwidth to ensure low-noise operation.

B. Electrical Characterization

To characterize the EGFET analog frontend circuit, a source-measure unit (SMU) was used to inject known currents into the device or emulate an electrochemical cell potential. Specifically, response to an emulated cell potential was observed by placing a variable isolated voltage source between both cell terminals, and recording the response, as the device applied constant bias potentials to the cell terminal (V_{Cell}), FET drain (V_{DS}), and TIA bias input (V_{Bias}). Next, I_D transduction was evaluated by shorting both cell terminals of a given channel together, while I_D was simultaneously measured using an SMU and the device's analog frontend circuit.

C. Electrode Functionalization

All reagents were commercially sourced. All solutions are prepared using DI water unless otherwise noted. All single-electrode potentials are relative to a Ag|AgCl reference. 10 mm x 6 mm planar gold electrodes were functionalized for NPY detection as follows [22]: first, sequential cleaning was performed with acetone, methanol, and isopropyl alcohol (IPA) for 30 seconds each, followed by 1 min O_2 plasma ashing. Cleaned electrodes were cleaned with cyclic voltammetry (CV, 12 cycles, 100 mV/s, -1 V to 1.3 V) in 0.5 M H_2SO_4 using a potentiostat. Cleaned electrodes were submerged in a solution of 1 µM thiolated anti-NPY aptamer [23] and 200 µM tris(2-carboxyethyl)phosphine hydrochloride (TCEP) in TE buffer overnight, then incubated for 1 h in 1 mM polyethylene glycol thiol, in darkness at room temperature. Electrodes were then rinsed with DI water and dried with N_2 prior to use. 2 mm diameter gold disk electrodes were functionalized for insulin detection as follows: first, electrodes were polished in an alumina suspension, then cleaned through sonication and incubation in piranha solution for 15 min each, followed by CV (20 cycles, 50 mV/s, -1.2 V to -0.2 V) in 50 mM KOH. Self-assembled monolayer (SAM) formation was achieved through overnight incubation in 100 µM dithiobis(succinimidyl hexanoate) (DSH) in acetone. Finally, electrodes were incubated in 0.05 mg/mL anti-insulin IgG (C7C9, Invitrogen) in PBS overnight at 4°C, followed by blocking against non-specific binding through incubation with 1 mM 6-mercapto-1-hexanol and 1 mM ethanolamine, for 1 h each in PBS. Electrodes were stored in PBS at 4°C until use. 10 mm x 6 mm planar gold electrodes were prepared for pH measurement through sequential cleaning with acetone, methanol, and IPA (30 seconds each) followed by 1 min O_2 plasma ashing. Next, polyaniline (PANI) was electrodeposited using CV (30 cycles, 100 mV/s, 1 V to -0.2 V) in a 0.1 M aniline solution with stirring. PANI electrodes were dried and cured at 80°C for 5 min. Electrodes were stored in desiccant at 80°C until use.

D. In Vitro Quantification

Electrodes were tested using the custom analog frontend circuit, as well as one of two "known-good" benchtop systems: either two SMUs (providing the electrochemical cell bias and FET drain bias, respectively), or a two-channel potentiostat.

For all analytes, the on-board FET was first disconnected from the frontend circuit and connected to the benchtop system. While the drain bias was held constant at 0.5 V, the cell bias potential was swept from -0.2 V to 1 V until a stable I-V curve was obtained. Analyte measurements were first obtained using the benchtop system (averaged over 4 sweeps) then using the reconnected analog frontend circuit. Holding the drain-source bias at 0.5 V and applying a fixed cell bias (either 0.6 V or 0.9 V), measurements were taken 10 seconds after application of bias potentials. After measurement in buffer, stock solution was

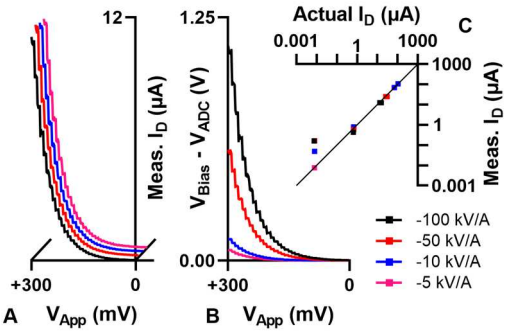

Fig. 2. Electrical characterization of EGFET frontend circuit. ADC output in response to an emulated cell voltage, given as A) transduced FET drain current (data staggered for visibility) and B) raw ADC output voltage with TIA bias voltage removed, for various TIA gain settings. V_{App} increased in 10mV steps. C) FET drain current transduced by the frontend circuit vs. simultaneous benchtop system measurement (log scale). V_{Cell} = 0.6 V, V_{DS} = 0.5 V, V_{Bias} = 1.25 V.

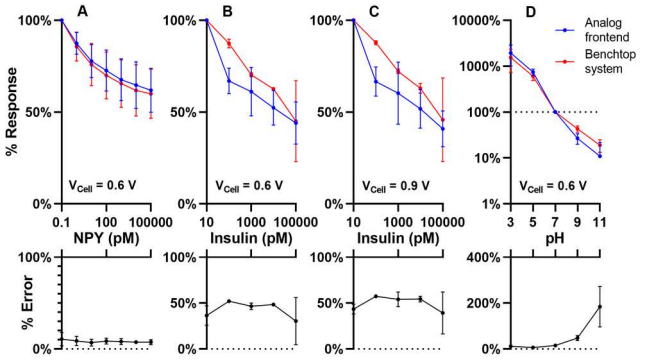

Fig. 3. In vitro measurement of A) NPY (n = 4), B,C) insulin (V_{Cell} = 0.6 V and 0.9 V, respectively, n = 2 each), and D) pH (n = 4), showing current transduced by the frontend circuit (blue) vs. current measured by benchtop system (red). Upper panel of each subfigure shows % current response, normalized to the lowest concentration in each series (NPY and insulin) or a neutral pH. Bottom panel of each subfigure shows % error (|observed – actual| / actual x 100%) taking frontend measurement as "observed" current and benchtop system measurement as "actual" current.

added to achieve the next target concentration, and after 5 min of equilibration the process was repeated, continuing until the full concentration series had been tested.

III. Results and Discussion

A. Electrical Characterization

Performance data for a simulated electrochemical cell demonstrated faithful reproduction of transduced I_D at all TIA gain settings, which scaled as expected for FET operation over a wide range of potentials applied between the device cell terminals (V_{App}, **Fig. 2A**). Raw TIA output voltages captured by the system's ADC scaled as expected based on selected TIA gain (**Fig. 2B**). Further, comparison between I_D values transduced by the system's TIA and simultaneous ground-truth measurements revealed a high degree of I_D transduction accuracy, except for small I_D values (~10 nA) for a subset of gain settings (**Fig. 2C**).

B. In Vitro Sensing Demonstration

Sequential measurements taken *in vitro* using the EGFET frontend circuit and ground-truth benchtop instruments revealed a high degree of correspondence between both measurement systems (**Fig. 3**). In all cases, both systems were able to track changes in analyte concentration (or pH) over the full supraphysiological range tested. Inter-electrode variability remains a concern, the severity of which can vary between specific functionalization schemes and recognition element types, *e.g.* aptameric sensors versus antibody-based sensors. Importantly, electrode-specific trends were observed to be nearly identical between our device and the benchtop instruments used, indicating this is not a limitation specific to the transduction circuit used.

Analyte sensitivity over each tested range was observed to be similar when detection was performed using either benchtop instruments or the EGFET frontend circuit (**Table 1**). For measurements of both NPY and pH, in which our system was compared against benchtop SMUs, measured percent error was typically under 10%, with the exception of measurements of alkaline solutions (pH 9 and especially pH 11, **Fig. 3D**). In the latter cases, measured I_D was close to or exceeded the lower bound of measurable current based on the TIA feedback resistors selected and effective ADC resolution (i.e., the FET was in extreme cutoff at these points). In practice, this issue could be ameliorated through the selection of larger feedback resistors if such small currents are anticipated as part of the analyte range of interest. Alternatively, our device's ability to provide a variable bias potential (V_{Cell}) to the electrochemical cell offers another method for addressing this limitation, through shifting the effective V_{GS} bias point (affected by both V_{Cell} and the working electrode junction potential, which is dependent on analyte concentration) closer to the transistor's intrinsic V_{th}. In the case of insulin quantification (**Fig. 3B,C**), in which our device was compared against a 2-channel potentiostat, measured percent error was somewhat larger (~50%), possibly due to a greater difference in intrinsic systematic offset between the two systems. Notably, measured percent error was approximately constant relative to both "known-good" instruments, within the valid ADC range.

Insulin quantification was demonstrated using two different cell biasing conditions (V_{Cell} = 0.6 V and V_{Cell} = 0.9 V), which produced nearly identical responses. Importantly, this demonstrates that V_{Cell} can be varied independently of the TIA gain setting as an additional method of varying the dynamic range of our device, including values both above and below the FET V_{th} (measured to be ~0.75 V in this case).

IV. Future Work

Future work is aimed at three main objectives: miniaturization through improved device integration and removal of unneeded features (relative to specific applications); extension of the device's dynamic range through increased voltage span (*e.g.* ±10 V rather than 0 V – 2.5 V); and validation with additional electrode-analyte systems.

TABLE 1

Sensitivity	NPY	Insulin (0.9 V V_{Cell})	pH
Bench inst.	-1.20 μA/dec.	-18.8 μA/dec.	-0.24 μA/pH
Frontend	-0.86 μA/dec.	-10.3 μA/dec.	-1.06 μA/pH

REFERENCES

[1] R. Fan and T. L. Andrew, "Perspective—Challenges in Developing Wearable Electrochemical Sensors for Longitudinal Health Monitoring," *Journal of The Electrochemical Society,* vol. 167, no. 3, p. 037542, 2020/01/20 2020, doi: 10.1149/1945-7111/ab67b0.

[2] D. M. Hilty, C. M. Armstrong, A. Edwards-Stewart, M. T. Gentry, D. D. Luxton, and E. A. Krupinski, "Sensor, Wearable, and Remote Patient Monitoring Competencies for Clinical Care and Training: Scoping Review," (in eng), *J Technol Behav Sci,* vol. 6, no. 2, pp. 252-277, 2021, doi: 10.1007/s41347-020-00190-3.

[3] E. R. Kim, C. Joe, R. J. Mitchell, and M. B. Gu, "Biosensors for healthcare: current and future perspectives," *Trends in Biotechnology,* vol. 41, no. 3, pp. 374-395, 2023/03/01/ 2023, doi: https://doi.org/10.1016/j.tibtech.2022.12.005.

[4] J. Tu, R. M. Torrente-Rodríguez, M. Wang, and W. Gao, "The Era of Digital Health: A Review of Portable and Wearable Affinity Biosensors," *Advanced Functional Materials,* vol. 30, no. 29, p. 1906713, 2020/07/01 2020, doi: https://doi.org/10.1002/adfm.201906713.

[5] R. W. Burnett *et al.*, "Use of ion-selective electrodes for blood-electrolyte analysis. Recommendations for nomenclature, definitions and conventions. International Federation of Clinical Chemistry and Laboratory Medicine (IFCC). Scientific Division Working Group on Selective Electrodes," (in eng), *Clin Chem Lab Med,* vol. 38, no. 4, pp. 363-70, Apr 2000, doi: 10.1515/cclm.2000.052.

[6] T. M. Drake and V. Gupta, "Calcium," in *StatPearls*. Treasure Island (FL) ineligible companies. Disclosure: Vikas Gupta declares no relevant financial relationships with ineligible companies.: StatPearls Publishing

[7] R. Pratiwi *et al.*, "A Review of Analytical Methods for Codeine Determination," (in eng), *Molecules,* vol. 26, no. 4, Feb 4 2021, doi: 10.3390/molecules26040800.

[8] L. Shaw and L. Dennany, "Applications of electrochemical sensors: Forensic drug analysis," *Current Opinion in Electrochemistry,* vol. 3, no. 1, pp. 23-28, 2017/06/01/ 2017, doi: https://doi.org/10.1016/j.coelec.2017.05.001.

[9] R. Asaf and S. Blum, "Applications of Electrochemistry in the Design and Development of Medical Technologies and Devices," in *Applications of Electrochemistry in Medicine*, M. Schlesinger Ed. Boston, MA: Springer US, 2013, pp. 35-53.

[10] H. Teymourian, A. Barfidokht, and J. Wang, "Electrochemical glucose sensors in diabetes management: an updated review (2010–2020)," *Chemical Society Reviews,* 10.1039/D0CS00304B vol. 49, no. 21, pp. 7671-7709, 2020, doi: 10.1039/D0CS00304B.

[11] V. D. Funtanilla, P. Candidate, T. Caliendo, and O. Hilas, "Continuous Glucose Monitoring: A Review of Available Systems," (in eng), *P t,* vol. 44, no. 9, pp. 550-553, Sep 2019.

[12] I. Lee, D. Probst, D. Klonoff, and K. Sode, "Continuous glucose monitoring systems - Current status and future perspectives of the flagship technologies in biosensor research," (in eng), *Biosens Bioelectron,* vol. 181, p. 113054, Jun 1 2021, doi: 10.1016/j.bios.2021.113054.

[13] J.-C. Chen, J.-C. Chou, T.-P. Sun, and S.-K. Hsiung, "Portable urea biosensor based on the extended-gate field effect transistor," *Sensors and Actuators B: Chemical,* vol. 91, no. 1, pp. 180-186, 2003/06/01/ 2003, doi: https://doi.org/10.1016/S0925-4005(03)00161-8.

[14] M. Krause *et al.*, "Extended gate electrode arrays for extracellular signal recordings," *Sensors and Actuators B: Chemical,* vol. 70, no. 1, pp. 101-107, 2000/11/01/ 2000, doi: https://doi.org/10.1016/S0925-4005(00)00568-2.

[15] J. van der Spiegel, I. Lauks, P. Chan, and D. Babic, "The extended gate chemically sensitive field effect transistor as multi-species microprobe," *Sensors and Actuators,* vol. 4, pp. 291-298, 1983/01/01/ 1983, doi: https://doi.org/10.1016/0250-6874(83)85035-5.

[16] A. M. Khalifa, S. A. Abdulateef, E. A. Kabaa, N. M. Ahmed, and F. A. Sabah, "Study of acidosis, neutral and alkalosis media effects on the behaviour of activated carbon threads decorated by zinc oxide using extended gate FET for glucose sensor application," *Materials Science in Semiconductor Processing,* vol. 108, p. 104911, 2020/03/15/ 2020, doi: https://doi.org/10.1016/j.mssp.2019.104911.

[17] S. Palit, K. Singh, B.-S. Lou, J.-L. Her, S.-T. Pang, and T.-M. Pan, "Ultrasensitive dopamine detection of indium-zinc oxide on PET flexible based extended-gate field-effect transistor," *Sensors and Actuators B: Chemical,* vol. 310, p. 127850, 2020/05/01/ 2020, doi: https://doi.org/10.1016/j.snb.2020.127850.

[18] S. Sheibani *et al.*, "Extended gate field-effect-transistor for sensing cortisol stress hormone," *Communications Materials,* vol. 2, no. 1, p. 10, 2021/01/19 2021, doi: 10.1038/s43246-020-00114-x.

[19] D. Probst, J. Twiddy, M. Hatada, S. Pavlidis, M. Daniele, and K. Sode, "Development of Direct Electron Transfer-Type Extended Gate Field Effect Transistor Enzymatic Sensors for Metabolite Detection," *Analytical Chemistry,* 2024/02/26 2024, doi: 10.1021/acs.analchem.3c04599.

[20] U. Tural and D. V. Iosifescu, "Neuropeptide Y in PTSD, MDD, and chronic stress: A systematic review and meta-analysis," *Journal of Neuroscience Research,* vol. 98, no. 5, pp. 950-963, 2020/05/01 2020, doi: https://doi.org/10.1002/jnr.24589.

[21] M. Hatada, S. Pavlidis, and K. Sode, "Development of a glycated albumin sensor employing dual aptamer-based extended gate field effect transistors," *Biosensors and Bioelectronics,* vol. 251, p. 116118, 2024/05/01/ 2024, doi: https://doi.org/10.1016/j.bios.2024.116118.

[22] H. Richardson, G. Maddocks, K. Peterson, M. Daniele, and S. Pavlidis, "Toward Subcutaneous Electrochemical Aptasensors for Neuropeptide Y," in *2021 IEEE Sensors*, 31 Oct.-3 Nov. 2021 2021, pp. 1-4, doi: 10.1109/SENSORS47087.2021.9639832.

[23] S. D. Mendonsa and M. T. Bowser, "In Vitro Selection of Aptamers with Affinity for Neuropeptide Y Using Capillary Electrophoresis," *Journal of the American Chemical Society,* vol. 127, no. 26, pp. 9382-9383, 2005/07/01 2005, doi: 10.1021/ja052406n.